

# Reverse Osmosis and Water Purification: Process and Procedures

Alexander Illarionov

March 8, 2016

## 1 Introduction

Hyperfiltration, or reverse osmosis, is the method of water purification using mechanical pressure to force the solvent from the region of high solute concentration, through a semipermeable membrane, to the region of low solute concentration. In the present practical investigation, experiments have been conducted to establish the relation between the properties of the NaCl solution being filtered and the effectiveness of osmotic purification.

## Notation

$J$  – molar flux [ $\text{mol m}^{-2} \text{ s}^{-1}$ ]

$J_v$  – volumetric flux, the rate of volume flow across a unit area [ $\text{m s}^{-1}$ ]

$L$  – phenomenological coefficient [ $\text{mol m}^{-1} \text{ W}^{-1} \text{ s}^{-2}$ ]

$\Delta p$  – pressure difference between the solution and water [ $\text{Pa}$ ]

$\Delta\pi$  – osmotic pressure of the solution, [ $\text{Pa}$ ]

## 2 Process

### 2.1 Theoretical Background

Consider a *perfect* semipermeable membrane, permeable to a solvent and completely impermeable to salt. Suppose such a membrane separates a salt solution of known concentration from pure water. The pressure on water is not necessarily equal to the pressure on the solution.

There are three cases:

1. the pressure difference between the solution and water,  $\Delta p$ , is lower than the osmotic pressure of the solution,  $\Delta\pi$ :

$$\Delta p < \Delta\pi$$

2. the osmotic equilibrium is established – no flow:

$$\Delta p = \Delta\pi$$

3. the water pressure dominates over the osmotic pressure:

$$\Delta p > \Delta\pi$$

Water flows from the solution into pure water. Thus, *reverse osmosis* is established.

An *imperfect* membrane is permeable to a solute. The hydrated salt usually flows from the region of high concentration to the region of low concentration. Therefore, as the pressure balance shifts from 1 to 3, the water flow is reversed, but not the flow of the solute. Let the molar flux of the hydrated salt be denoted as  $J_s$ , and let the molar flux of the water be  $J_w$ . Let their driving forces be  $F_s$  and  $F_w$  respectively. In general, these fluxes interact so that they can be expressed as functions of their driving forces, where  $L_{ij}$  for  $i, j \in \{1, 2\}$  are phenomenological

coefficients obtained empirically[3]:

$$J_s = L_{12}F_w + L_{11}F_s \quad (1)$$

$$J_w = L_{21}F_s + L_{22}F_w \quad (2)$$

These equations are valid in theory for sufficiently small deviations from osmotic equilibrium. The Onsager reciprocity relation ensures that  $L_{12} = L_{21}$ . Thus, the reverse osmosis system can be described by three independent variables. The transport coefficients  $L_{ij}$  usually vary greatly with the concentration of the observed species.[3]

Reverse osmosis can also be described as a thermodynamical process. The thermodynamical treatment depends on the notion that at equilibrium the chemical potential of the solvent must be the same on both sides of the semipermeable membrane. Thus, as the chemical potential of the solvent is lowered by the solute, it must be restored to the original value by the osmotic pressure applied to retain equilibrium. This in turn implies that for *dilute* solutions the osmotic pressure can be modelled by the *van't Hoff equation*[1]:

$$\Delta\pi = iCRT, \quad (3)$$

where  $i$  is the ratio of the number of non-solvent particles in solution to the quantity of the solute dissolved (for NaCl,  $i = 2$ ),  $C$  is the molar concentration of the solute,  $R$  is the ideal gas constant, and  $T$  is the absolute temperature of the solution. Thus, in the solute-solvent equilibrium at constant temperature the osmotic pressure is directly proportional to the molar concentration of the solute.

Vapour pressure bears a significant effect on the vapour-liquid equilibrium, and vice versa. The vapour-liquid equilibrium is also affected by the solutes and their interaction with the liquid as a solvent. ([1],[2]) The relation between the ratio of vapour pressures in solution and

pure liquid and composition of the liquid  $A$  is given by Raoult's law:

$$p_A = x_A p_A^* \quad (4)$$

If the components of the mixture are structurally similar, the model of Raoult's law gives very accurate predictions. [1] Solutions that obey Raoult's law are called *ideal*. In ideal solutions both the solute and the solvent can be described by Raoult's model. In real solutions of low concentrations, however, it was found experimentally that, even if the vapour pressure of the solute is proportional to its mole fraction, the constant of proportionality may differ from the vapour pressure of the pure liquid. This empirical fact is expressed in Henry's law:

$$p_B = x_B K_B , \quad (5)$$

where  $x_B$  is the mole fraction of the solute  $B$  and  $K_B$  is an empirical constant.

Mixtures which solutes can be described by Henry's law and which solvents can be modelled by Raoult's law are called *ideal-dilute solutions*. When a solute is introduced into an ideal-dilute solution, the chemical potential of the solvent  $A$  drops from some value  $\mu_A^*$  to  $\mu_A^* + RT \ln x_A$  [1]. Notice that there is no direct effect of the solute on the vapour pressure of the solvent, provided the solute is neither solid nor gaseous, which is the case with NaCl in solution. The reduction of the chemical potential, however, shifts the equilibrium to a higher temperature (i.e. the boiling point is increased) and the solid-liquid equilibrium to a lower temperature (i.e. the freezing point is decreased). The water flux through the membrane rises. Therefore, measuring how the vapour pressure of the solution changes can give clues about the nature of the osmotic equilibrium.

### 3 Procedures

#### 3.1 Materials

Consumables:

- tap & distilled water
- salt

Equipment:

- electronic balance
- logging pressure sensor
- stopwatches
- hot-plate magnetic stirrer
- graduated cylinders and beakers
- burettes
- teat pipette
- dialysis tubing
- chemical splash safety goggles
- gloves
- rubber bands and threads

#### 3.2 Safety Precautions

*NaCl:*

Dry or dissolved NaCl may cause eye, skin, gastrointestinal (on ingestion), and respiratory

tract (on inhalation) irritation. Salt must be used with adequate ventilation, and access to an eyewash facility must be maintained at all times. Safety glasses, gloves, and aprons may be worn.

*Electronics:*

To avoid damage to instruments and electric shock, keep hands dry and place all the equipment in contact with water inside spill-proof plastic trays.

### 3.3 Preliminary Experimental Work

To obtain empirical evidence that the reverse osmosis is viable with the equipment described in the section 3.1, two rough trials were conducted:

1. The samples of salt were weighted on the electronic balance in different beakers to give  $30.02 \pm 0.01$  g and  $40.95 \pm 0.01$  g.
2. Solutions of volume  $300 \pm 1$  cm<sup>3</sup> were prepared using the hot-plate magnetic stirrer.
3. Two dialysis tubings were sealed with a knot on the bottom and a standard 1 mm thread, attached to the burettes with the thread and then filled with the solutions.
4. The tubings were then immersed into distilled water and changes in the volumes were timed using two stopwatches.

The results are recorded in Table 3 and 4 on pages 16 and 17.

The graph of the preliminary experiment is given on page 7. The result is unexpected, since the solution of higher concentration was said to exhibit greater osmotic pressure, and hence the flux must be greater for the 2.34 M solution, which is not supported by the data, since the gradient of volumetric change for the 1.71 M solution is greater at all times. One of the reasons why this was the case became clear when both tubings were taken out of the beaker; the first tubing was leaking due to the incomplete attachment to the burette and poor fixation of the bottom. Moreover, the membranes had different dimensions, with the leaking tubing being 2.2

cm × 12 cm in width and length versus 2.7 cm × 16 cm of the non-leaking membrane.

There were several improvements to make:

1. Membranes of similar dimensions must be used.

Please note the word 'similar'. Since the tubings are eventually twisted and squeezed, the precise homogeneity of the surface between any two samples is difficult to attain with the instruments available.

2. More reliable fixating tools must be used.

The standard thread, 1 mm in width, was not strong enough.

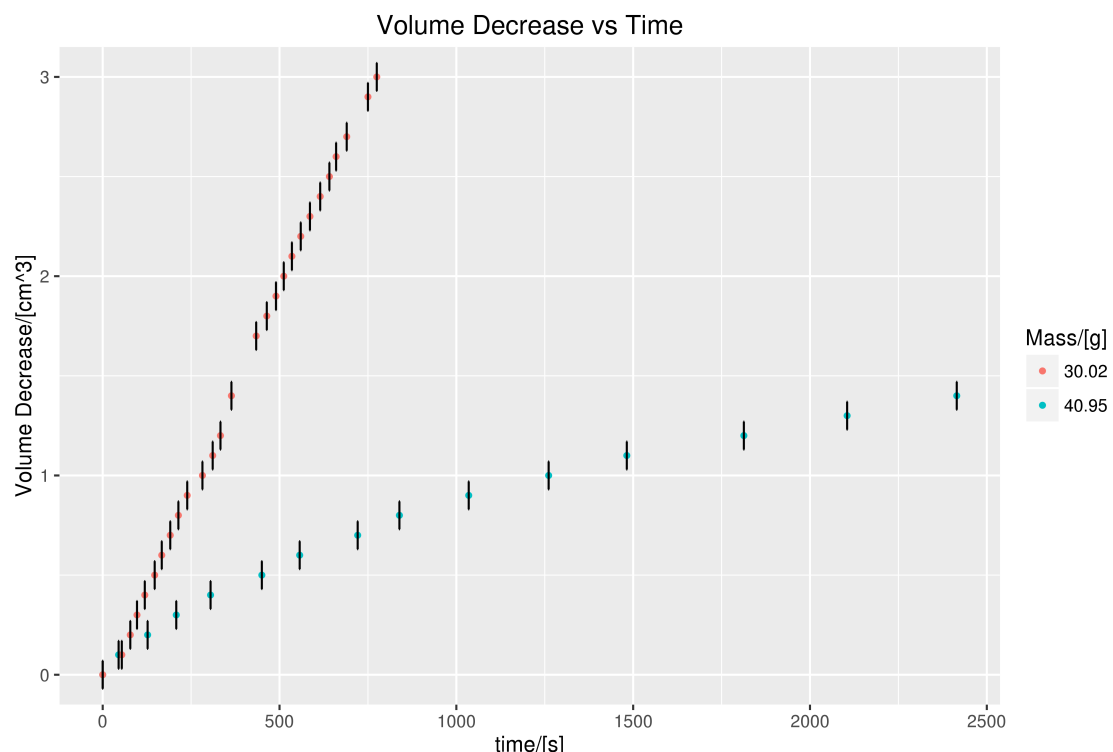


Figure 1: The graph of the trial experiment with the  $1.71 \pm 0.01$  M and  $2.34 \pm 0.01$  M solutions, corresponding to the mass of 30.02 g and 40.95 g of added salt.

### 3.4 Progress

The same method was applied to obtain the data for the solutions with the masses of added salt equal to  $10.34 \pm 0.01$  g,  $20.72 \pm 0.01$  g and  $36.72 \pm 0.01$  g. The membranes were all cut to the same initial dimensions of  $2.2\text{ cm} \times 12\text{ cm}$ . It was found that neither standard thread applied in excess nor the thread coupled with rubber bands were completely effective in preventing the dialysis membranes from leaking, presumably due to a significant push from the water column in the burette. Thus, a new thread of width  $3 \pm 1$  mm was utilised, which substantially easened the procedure of both attaching the tubing to the burette and blocking the flow of water from the bottom. Double knots were applied to the bottom of the Visking tubing as well.

Please find the corresponding results recorded in tables 5, 6, 7 on pages 18, 19.

#### 3.4.1 Measuring Change in Pressure

Following the discussion of the vapour pressure and how it relates to the osmotic pressure in section 2.1, measuring change in vapour pressure can give us more information about how the concentration affects the process of reverse osmosis. To achieve this, a pressure sensor with precision of up to 1 Pa was left logging data over long periods of time for solutions with  $19.12 \pm 0.01$  g,  $19.98 \pm 0.01$  g and  $43.37 \pm 0.01$  g of salt dissolved in  $300 \pm 1\text{ cm}^3$ , corresponding to  $1.09 \pm 0.01$  M,  $1.14 \pm 0.01$  M and  $2.47 \pm 0.01$  M solutions respectively. (if all the resultant quotient uncertainties are ceiled). The setup is given in the figure 2 below.

Starting with  $1.09 \pm 0.01$  M solution, two rough trials showed the necessity of stabilising the sensor by using the clamp and clamp stand due to the random fluctuations resulting from the irregular movement of the sensor tubes. These were fixed shortly afterwards. The experiment was continued overnight. The next day the concentration was changed to  $1.14 \pm 0.01$  M and the setup was left running for a weekend. The concentration was changed to  $2.47 \pm 0.01$  M on Monday and left overnight. On Tuesday it was found that the tubing with the 2.47 M solution was very easy to break. Therefore, microholes could have developed in the membrane which subjected the tubing to leaking.

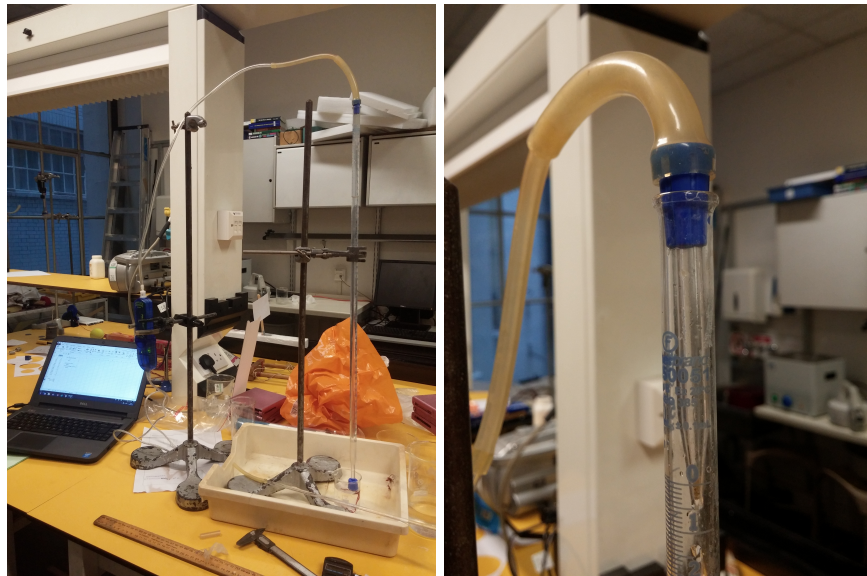


Figure 2: The reverse osmosis setup with the pressure sensor. Note that the sensor and its tubes rest on the clamps to reduce random pressure fluctuations.

1214181 data points were collected by the pressure sensor in total. These are represented in the graph of the pressure change against time on page 10.

The volumetric decrease was measured concurrently during lab hours. These are presented in the tables 8, 9, 10. All the volumetric change data recorded during the experiment is shown in the graph 4 on page 11.

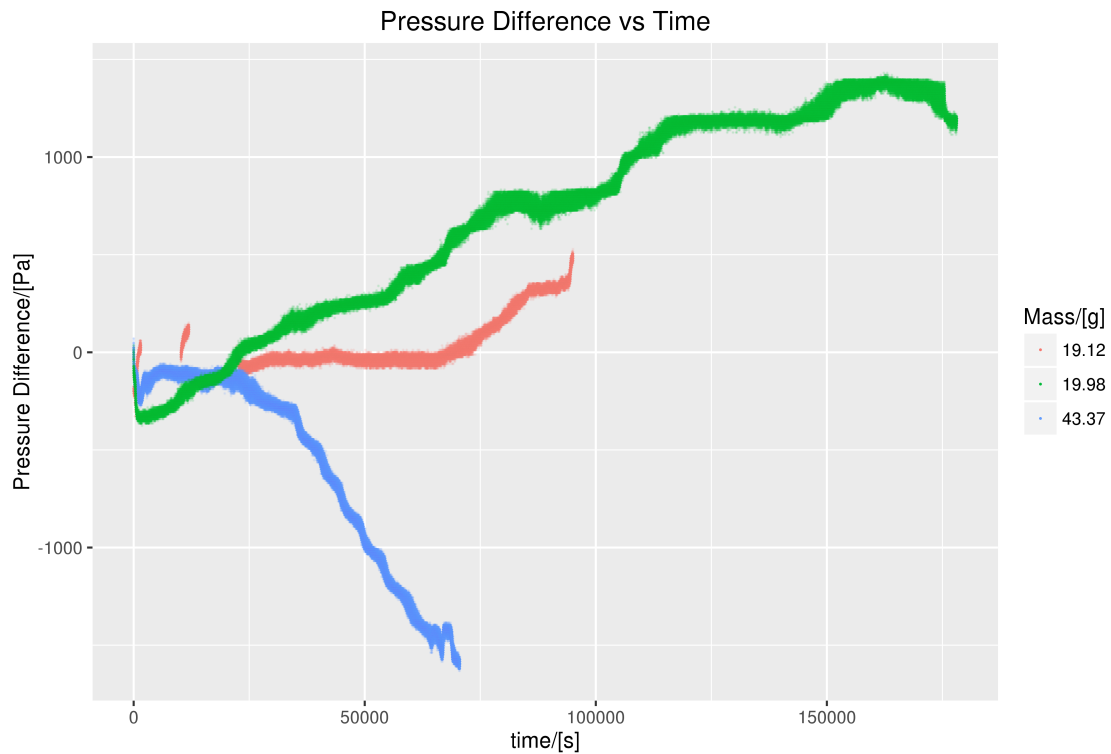


Figure 3: The pressure change relative to the absolute pressure at the start of the experiment is represented. Please note that the line corresponding to  $m_0(NaCl) = 19.12\text{ g}$  has two gaps – these were the breaks after trial runs, during which the sensor was clamped on the stand. Notice also that the random fluctuation of data exceeds the instrument uncertainty, hence, to avoid cluttering, it is not shown.

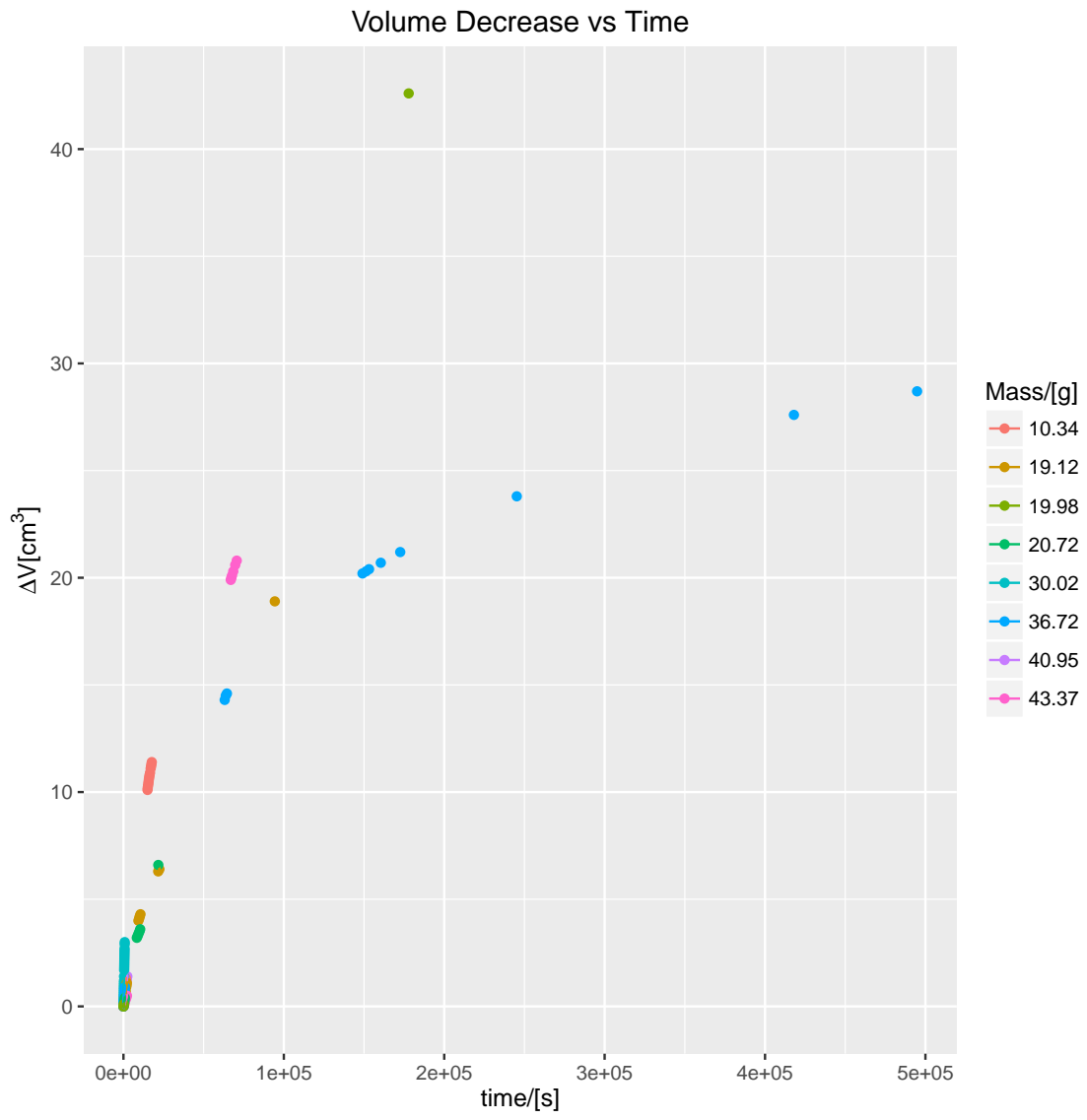


Figure 4: The volume decrease plotted against time. Notice that there are no error bars – they are insignificant relative to the orders of magnitudes involved.

### 3.5 Analysis

#### 3.5.1 Volume Decrease

Consider the graph 4. Let  $m$  be the mass of the salt in the original solution in grams. The best piece of visual evidence for the existence of some model describing the relationship between  $\Delta V$  and  $t$  is given by  $m = 36.72$ . The shape of the plot for  $m = 36.72$  strongly suggests there is a well-defined trend in the bivariate distribution of  $\Delta V$  and  $t$ .

Let's introduce a coefficient called *mass inflow factor*  $\mu$ , or MIF. Define  $\mu$  as  $\frac{1}{m - \rho_w \Delta V}$ , where  $\rho_w$  is the density of water. I argue that  $\mu \sim \gamma + \phi t$  for some constants  $\phi$  [ $\text{g}^{-1} \times \text{s}^{-1}$ ] and  $\gamma$  [ $\text{g}^{-1}$ ] if  $m$  is sufficiently greater than  $\rho_w \Delta V$ .  $\rho_w$  is equal to  $1.0 \text{ g} \times \text{cm}^{-3}$  (2 s.f.).

The following are some properties of  $\mu$  as a linear function of  $t$ :

1. If at  $t = 0$   $\Delta V = 0$ ,  $\mu|_{t=0} = m^{-1} = \gamma$
2.  $\mu$  is undefined at  $t = \tau$  such that  $\Delta V(\tau) = \frac{m}{\rho_w}$
3.  $\mu$  changes sign in the neighbourhood of  $t = \tau$
4.  $\mu$  approaches zero from below if  $\Delta V$  is unbounded from below as  $t \rightarrow \infty$  (if, for instance, there is a hole in the membrane).

Consider  $\mu|_{m=36.72}$ . The statistics associated with the regression line are calculated using R `lm()` and `summary()` methods; the results are given in the table 1.

Table 1: The Regression Model for  $\mu|_{m=36.72}$

	Estimate	Std. Error	t-value	Pr(> t )
(Intercept)	2.77E-02 $\text{g}^{-1}$	9.84E-04 $\text{g}^{-1}$	2.82E+01	1.06E-15
t	2.02E-07 $\text{g}^{-1} \times \text{s}^{-1}$	5.47E-09 $\text{g}^{-1} \times \text{s}^{-1}$	3.70E+01	1.07E-17

In the first column, the (Intercept) corresponds to the modelled  $\gamma$ , while t is the modelled value of  $\phi$ . The t-value corresponds to the t-statistic, and the last column shows the probability of getting such a value of  $\phi$  by pure chance. As can be seen from the data, such a probability is small.

Our analysis can be repeated for other values of  $m$ . To ensure that  $m$  is sufficiently greater than  $\rho_w \Delta V$ , our Volumetric Decrease data set was sorted to include only those values for which  $m - 1 > \rho_w \Delta V$ . To exclude false positives due to insufficient data,  $m=19.18$  was excluded. Then the linear regression models were computed, which fit the data well, as shown by low values of variance. The result given in the table 2 is also represented in the Figure 5 on 14.

Table 2: Linear Regression Modelling of MIF vs Time

$m, g$	$\phi, (g \times s)^{-1}$	$\sigma_\phi, (g \times s)^{-1}$	$\gamma, g^{-1}$	$\sigma_\gamma, g^{-1}$
10.34	8.33E-06	1.75E-07	9.69E-02	1.64E-04
19.12	1.23E-06	3.91E-08	5.28E-02	3.53E-04
20.72	1.03E-06	1.26E-08	4.82E-02	1.15E-04
30.02	4.95E-06	4.24E-08	3.32E-02	1.89E-05
36.72	1.97E-07	3.47E-09	2.92E-02	6.25E-04
40.95	3.47E-07	2.24E-08	2.45E-02	2.61E-05
43.37	2.99E-07	1.65E-09	2.29E-02	7.99E-05

Since at  $t = 0$   $\Delta V$  was always zero, the dependence of MIF on time can be described as follows:

$$\frac{\frac{\rho_w \Delta V}{m}}{\rho_w \Delta V - m} = -\phi t \quad (6)$$

### 3.5.2 Vapour Pressure

A distinct feature of the graph 3 is the intersection of three curves at  $t \approx 20000$  s. After this point their characters differ considerably. The nature of the graph corresponding to  $m = 19.12$  g was significantly affected by the breaks for tuning: the initial steep pressure gradient became shallower, the liquid-vapour equilibrium was disrupted and took time to reestablish itself. Note that the initial conditions before the new equilibrium are drastically different from the initial conditions of the experiment: after more than 60000 seconds passed the concentrations of the solutions on both sides of the semipermeable membrane have changed.

The plots corresponding to  $m = 19.98$  and  $m = 43.37$  are almost symmetrical in the horizontal line. 2.47 M solution, shown in blue, has a drastic effect on the chemical potential of the solution and hence on the osmotic pressure. The predominantly negative pressure change implies that there is not enough ambient energy in the chemical environment for the stable

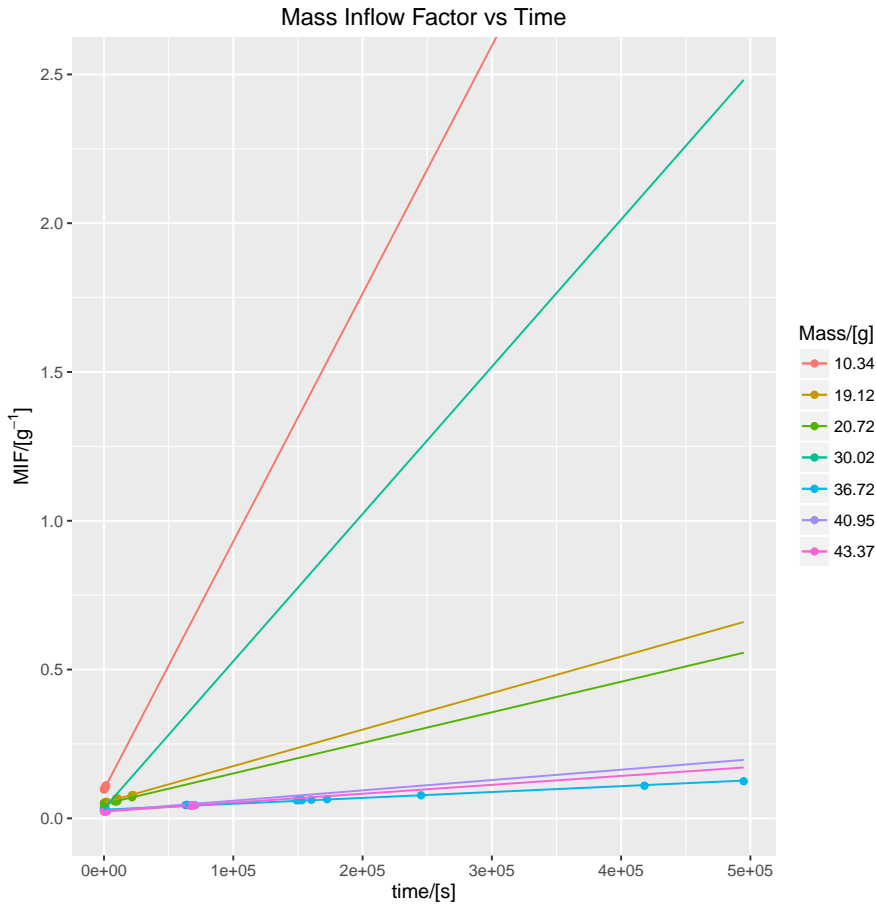


Figure 5: Notice that the position of the models for  $m$  equal to 30.02 g, 40.95 g and 43.37 g do not fit the trend of the greater  $\phi$  for lower  $m$ . The first two were used in the trial experiment with shoddy fixation, while the first and the last were later found leaking or on the verge of leaking.

equilibrium to form, although some degree of occasional stabilisation is visible in the staircase-like appearance of the graph. The same trend is visible in the form of the plot for the 1.14 M solution, shown in green. There, however, active vapourisation of the solvent seems to take place, which counteracts the changes in the volume available for the vapour. The overall rate of the pressure change is slower for the less concentrated solutions, which may be explained by the greater wear of the membrane due to faster osmotic interactions, as supported by the near-failure condition of the tubing at the end of the experiment.

## 4 Conclusion

Reverse osmosis is an exciting and challenging technique for water purification. Multitude factors must be taken into account when designing an efficient and durable osmotic system:

- concentration of the filtrated solution
- surface area and homogeneous texture of the membrane
- environmental conditions, such as the state of the vapour-liquid equilibrium, temperature and pressure

The relation between the mass of the dissolved salt and the volumetric flux was proposed. The accuracy of the equation and its independence from the specifics of the equipment or materials used must be carefully examined.

## 5 Tables

Please note that the absolute error of the volume change depends on two readings. The scale of the burette is  $0.1 \text{ cm}^3$ , hence the total uncertainty in the volume change value is  $\sqrt{2 \times (\frac{0.1}{2})^2} \approx 0.07 \text{ cm}^3$ .

Table 3: Volume Change with Time for  $m = 30.02 \text{ g}$

	time[s]	$\varepsilon$ time[s]	$\Delta$ volume [ $\text{cm}^3$ ]	$\varepsilon$ volume [ $\text{cm}^3$ ]
1	0.00	1.00	0.00	0.07
2	54.00	1.00	0.10	0.07
3	78.00	1.00	0.20	0.07
4	97.00	1.00	0.30	0.07
5	119.00	1.00	0.40	0.07
6	147.00	1.00	0.50	0.07
7	167.00	1.00	0.60	0.07
8	191.00	1.00	0.70	0.07
9	214.00	1.00	0.80	0.07
10	239.00	1.00	0.90	0.07
11	282.00	1.00	1.00	0.07
12	311.00	1.00	1.10	0.07
13	333.00	1.00	1.20	0.07
14	364.00	1.00	1.40	0.07
15	434.00	1.00	1.70	0.07
16	464.00	1.00	1.80	0.07
17	490.00	1.00	1.90	0.07
18	512.00	1.00	2.00	0.07
19	535.00	1.00	2.10	0.07
20	560.00	1.00	2.20	0.07
21	586.00	1.00	2.30	0.07
22	615.00	1.00	2.40	0.07
23	641.00	1.00	2.50	0.07
24	660.00	1.00	2.60	0.07
25	690.00	1.00	2.70	0.07
26	750.00	1.00	2.90	0.07
27	775.00	1.00	3.00	0.07

Table 4: Volume Decrease with Time for  $m = 40.95$  g

	time[s]	$\varepsilon$	time[s]	$\Delta$ volume [ $\text{cm}^3$ ]	$\varepsilon$ volume [ $\text{cm}^3$ ]
1	0.00		1.00	0.00	0.07
2	45.00		1.00	0.10	0.07
3	127.00		1.00	0.20	0.07
4	208.00		1.00	0.30	0.07
5	305.00		1.00	0.40	0.07
6	450.00		1.00	0.50	0.07
7	557.00		1.00	0.60	0.07
8	721.00		1.00	0.70	0.07
9	839.00		1.00	0.80	0.07
10	1035.00		1.00	0.90	0.07
11	1261.00		1.00	1.00	0.07
12	1482.00		1.00	1.10	0.07
13	1813.00		1.00	1.20	0.07
14	2105.00		1.00	1.30	0.07
15	2415.00		1.00	1.40	0.07

Table 5: Volume Decrease with Time for  $m = 10.34$  g

	time[s]	$\varepsilon$ time[s]	$\Delta$ volume [cm $^3$ ]	$\varepsilon$ volume [cm $^3$ ]
1	0.00	1.00	0.00	0.07
2	45.00	1.00	0.10	0.07
3	155.00	1.00	0.20	0.07
4	307.00	1.00	0.30	0.07
5	452.00	1.00	0.40	0.07
6	614.00	1.00	0.50	0.07
7	731.00	1.00	0.60	0.07
8	868.00	1.00	0.70	0.07
9	967.00	1.00	0.80	0.07
10	1047.00	1.00	0.90	0.07
11	1253.00	1.00	1.00	0.07
12	1375.00	1.00	1.10	0.07
13	1488.00	1.00	1.20	0.07
14	1575.00	1.00	1.30	0.07
15	15005.00	1.00	10.10	0.07
16	15123.00	1.00	10.20	0.07
17	15330.00	1.00	10.30	0.07
18	15525.00	1.00	10.40	0.07
19	15691.00	1.00	10.50	0.07
20	15863.00	1.00	10.60	0.07
21	16077.00	1.00	10.70	0.07
22	16291.00	1.00	10.80	0.07
23	16555.00	1.00	10.90	0.07
24	16967.00	1.00	11.10	0.07
25	17212.00	1.00	11.20	0.07
26	17437.00	1.00	11.30	0.07
27	17659.00	1.00	11.40	0.07

Table 6: Volume Decrease with Time for  $m = 20.72$  g

	time[s]	$\varepsilon$ time[s]	$\Delta$ volume [cm $^3$ ]	$\varepsilon$ volume [cm $^3$ ]
1	0.00	1.00	0.00	0.07
2	309.00	1.00	0.10	0.07
3	493.00	1.00	0.20	0.07
4	684.00	1.00	0.30	0.07
5	875.00	1.00	0.40	0.07
6	8323.00	1.00	3.20	0.07
7	8922.00	1.00	3.30	0.07
8	9437.00	1.00	3.40	0.07
9	9999.00	1.00	3.50	0.07
10	10427.00	1.00	3.60	0.07
11	21725.00	1.00	6.60	0.07

Table 7: Volume Decrease with Time for  $m = 36.72$  g

	time[s]	$\varepsilon$	time[s]	$\Delta$ volume [cm $^3$ ]	$\varepsilon$ volume [cm $^3$ ]
1	0.00		1.00	0.00	0.07
2	75.00		1.00	0.10	0.07
3	144.00		1.00	0.20	0.07
4	241.00		1.00	0.30	0.07
5	426.00		1.00	0.50	0.07
6	657.00		1.00	0.70	0.07
7	812.00		1.00	0.80	0.07
8	967.00		1.00	0.90	0.07
9	63120.00		60.00	14.30	0.07
10	63780.00		60.00	14.50	0.07
11	64500.00		60.00	14.60	0.07
12	149040.00		60.00	20.20	0.07
13	151260.00		60.00	20.30	0.07
14	153120.00		60.00	20.40	0.07
15	160440.00		60.00	20.70	0.07
16	172560.00		60.00	21.20	0.07
17	245220.00		60.00	23.80	0.07
18	418020.00		60.00	27.60	0.07
19	494820.00		60.00	28.70	0.07

Table 8: Volume Decrease with Time for  $m = 19.12$  g

	time[s]	$\varepsilon$	time[s]	$\Delta$ volume [cm $^3$ ]	$\varepsilon$ volume [cm $^3$ ]
1	17.00		1.00	0.00	0.07
2	419.00		1.00	0.10	0.07
3	576.00		1.00	0.20	0.07
4	740.00		1.00	0.30	0.07
5	886.00		1.00	0.40	0.07
6	1068.00		1.00	0.50	0.07
7	1240.00		1.00	0.60	0.07
8	1403.00		1.00	0.70	0.07
9	1718.00		1.00	0.90	0.07
10	1958.00		1.00	1.00	0.07
11	2118.00		1.00	1.10	0.07
12	9328.00		1.00	4.00	0.07
13	9772.00		1.00	4.10	0.07
14	10169.00		1.00	4.20	0.07
15	10608.00		1.00	4.30	0.07
16	21667.00		1.00	6.30	0.07
17	22392.00		1.00	6.40	0.07
18	94368.00		1.00	18.90	0.07

Table 9: Volume Decrease with Time for  $m = 19.98$  g

	time[s]	$\varepsilon$ time[s]	$\Delta$ volume [cm $^3$ ]	$\varepsilon$ volume [cm $^3$ ]
1	55.00	1.00	0.00	0.07
2	161.00	60.00	0.10	0.07
3	177835.00	60.00	42.60	0.07

Table 10: Volume Decrease with Time for  $m = 43.37$  g

	time[s]	$\varepsilon$ time[s]	$\Delta$ volume [cm $^3$ ]	$\varepsilon$ volume [cm $^3$ ]
1	13.00	1.00	0.00	0.07
2	502.00	1.00	0.10	0.07
3	858.00	1.00	0.20	0.07
4	1242.00	1.00	0.30	0.07
5	1743.00	1.00	0.40	0.07
6	2177.00	1.00	0.50	0.07
7	66913.00	60.00	19.90	0.07
8	67273.00	60.00	20.00	0.07
9	67693.00	60.00	20.10	0.07
10	68473.00	60.00	20.30	0.07
11	69673.00	60.00	20.60	0.07
12	70633.00	60.00	20.80	0.07

## References

- [1] Atkins, P., and de Paula, J. *Atkins' Physical Chemistry*. Oxford University Press, New York, 2010.
- [2] Chaudry, M. A. Water and ions transport mechanism in hyperfiltration with symmetric cellulose acetate membranes. *Journal of membrane science* 206, 1 (2002), 319–332.
- [3] Spiegler, K., and Kedem, O. Thermodynamics of hyperfiltration (reverse osmosis) : criteria for efficient membranes. *Desalination* 1, 4 (1966), 311–326.